water

IMPACT FACTOR 3.0

CITESCORE 5.8

Article

Study of the Biogas Ebullition from Lacustrine Carbonate Enriched and Black Silt Bottom Sediments

Evaldas Maceika, Laima Kazakevičiūtė-Jakučiūnienė, Zita Žukauskaitė, Nina Prokopčiuk, Marina Konstantinova, Vadimas Dudoitis and Nikolay Tarasiuk

MDPI

https://doi.org/10.3390/w16243608

water

MDPI

Article

Study of the Biogas Ebullition from Lacustrine Carbonate Enriched and Black Silt Bottom Sediments

Evaldas Maceika [1,*], Laima Kazakevičiūtė-Jakučiūnienė [1], Zita Žukauskaitė [1], Nina Prokopčiuk [2], Marina Konstantinova [1], Vadimas Dudoitis [1] and Nikolay Tarasiuk [1]

[1] Center for Physical Sciences and Technology, Savanoriu Ave. 231, LT-02300 Vilnius, Lithuania; laima.kazakeviciute@ftmc.lt (L.K.-J.); zita.zukauskaite@ftmc.lt (Z.Ž.); marina.konstantinova@ftmc.lt (M.K.); vadimas.dudoitis@ftmc.lt (V.D.)

[2] Clinic of Children's Diseases, Institute of Clinical Medicine, Faculty of Medicine, Vilnius University, Antakalnio Str. 57, LT-10207 Vilnius, Lithuania; nina.prokopciuk@mf.vu.lt

* Correspondence: evaldas.maceika@ftmc.lt; Tel.: +370-65046440

Abstract: The greenhouse effect, which is also promoted by naturally occurring biogas ebullition fluxes (released via bubbles), generated by the decomposition of organic matter in carbonate-enriched and black silt sediments, has been analyzed. This study is based on results obtained using passive gas collectors at different parts of eutrophic Lake Juodis, located in a temperate climate zone in the vicinity of Vilnius (Lithuania). The measured annual biogas (containing about 60% of biomethane) ebullition fluxes from carbonate-enriched sediments and black silt sediments were 16.9–23.0 L/(m^2·y) and 38.5–43.2 L/(m^2·y), respectively. This indicates that the gas fluxes from carbonate sediments were almost twice as low as those from black silt sediments. Oxygen, produced by the photosynthetic activity of green algae in the near-surface water and sediments, helps to retain carbonates in the sediments by preventing their dissolution. In turn, the calcite coating on sediment particles partially preserves organic matter from decomposition, reducing the effective thickness of the sediment layer generating biogas. The characteristic vertical distribution profile of ^{137}Cs activity, with sharp peaks in sediments, suggests that generated biogas bubbles move to the surface of the sediments forming vertical channels by pushing sediment particles asides without noticeably mixing them vertically. This examination showed that factors such as abundance of carbonates in the sediments may result in a significant reduction in biogas generation and emissions from the lake sediments.

Keywords: greenhouse gas; biomethane ebullition; lake sediment mixing; ^{137}Cs

Citation: Maceika, E.; Kazakevičiūtė-Jakučiūnienė, L.; Žukauskaitė, Z.; Prokopčiuk, N.; Konstantinova, M.; Dudoitis, V.; Tarasiuk, N. Study of the Biogas Ebullition from Lacustrine Carbonate Enriched and Black Silt Bottom Sediments. *Water* **2024**, *16*, 3608. https://doi.org/10.3390/w16243608

Academic Editor: Achim A. Beylich

Received: 15 November 2024
Revised: 11 December 2024
Accepted: 13 December 2024
Published: 15 December 2024

1. Introduction

The Kyoto Protocol (2005) and the Paris Agreement (2016) are based on a scientific consensus that greenhouse gases (GHG), primarily carbon dioxide (CO_2), methane (CH_4), nitrous oxide (N_2O), hydrofluorocarbons (HFCs), perfluorocarbons (PFCs)), and emissions of sulfur hexafluoride (SF_6), are responsible for the current climate warming. Between 2030 and 2050, climate change is projected to cause a quarter of a million deaths per year [1]. Methane is the second most abundant greenhouse gas after carbon dioxide (CO_2), accounting for a significant portion of global GHG emissions [2]. Methane is emitted from a variety of anthropogenic (such as agriculture, forest fires, energy, and industry, as well as waste from homes and business) and natural sources. Natural sources such as wetlands (emitting CH_4 from bacteria that decompose organic material in the absence of oxygen), reservoirs and ponds (with high organic matter and low oxygen levels, producing methane through the microbial breakdown of organic matter), oceans, volcanoes, livestock, termites, and wildfires can generate large amounts of CH_4. Upon escaping into the atmosphere, greenhouse gases absorb energy and slow the rate at which heat leaves the planet. On a 100-year timescale, methane is more than 28 times (and up to 84 times over a 20-year timescale) as potent as carbon dioxide at trapping heat in the atmosphere and causing

climate change [3]. Lakes actively transform carbon and play a crucial role in both natural and anthropogenic greenhouse gas budgets, including carbon dioxide (CO_2) and methane (CH_4) [4–12]. The bottom sediments buffer and modulate biogas emissions (composed mostly of methane, carbon dioxide, and nitrogen) in aquatic systems, and these need to be considered in process-based models [4,13]. However, accurately estimating carbon budgets for lakes remains challenging due to the large spatial variability and the scarcity of data on the magnitude of CO_2 and CH_4 emissions from lakes on regional and global scales. Nutrients play a crucial role in affecting CO_2 and CH_4 levels in lakes. They can either reduce CO_2 net emissions by increasing primary productivity of plants or increase CO_2 and methane emissions by stimulating microbial activities that enhance respiration [12,14]. However, a range of the other characteristics of freshwater reservoirs can affect CH_4 emissions to the atmosphere [5,15–19]. Water depth has been found to be negatively correlated with emission rates and to control the relative contribution of the different emission pathways. Meanwhile, lake area, anoxic lake volume, temperature, and concentrations of total phosphorus and dissolved organic carbon were positively correlated with emission rates [18,20]. Another factor affecting CH_4 emissions is seasonality, which decreases in importance from boreal to temperate and tropical regions. In lakes with ice cover and stable summer stratification, emissions peak in spring and autumn, whereas in polymictic lakes, peaks occur in summer, with high temperatures and primary production suggested as major drivers of CH_4 emission [18,19,21].

Shallow waters, which are typical of urban areas, are likely to emit more CH_4 per unit of surface area, because the travel times of CH_4 bubbles are shorter, limiting CH_4 oxidation by methanotrophy in the oxic water column [18].

Methane is known to escape into the atmosphere via four major pathways: ebullition, surface diffusion, advection through plants, and the exposure of anoxic, CH_4-rich deep waters to the atmosphere during convective mixing events [3]. A study [7] indicates that the methane flux from sediments can be about nine times higher than the diffusion flux. Research has shown that the methane production rate in sediment columns can vary among layers, typically following a decreasing trend with depth [8,9]. Rothfuss and Conrad [22] performed laboratory experiments demonstrating that methane bubble formation in sediments begins at a depth of about 10 mm, with maximum bubble production occurring in the 11–17 mm depth range, gradually decreasing to zero at grater depths. Additionally, it was observed that the symbiotic structure of the microbial community in the early stage creates favorable conditions for CH_4 formation in sediments [23]. Bioturbation can significantly influence methane release from bottom sediments. Studies examining the effects of processes such as disturbance, bioturbation, and sediment microbial ecology on the heterogenous nature of methane emissions in various freshwater ecosystems have identified a linear relationship between decreased methanogen populations and increased disturbance frequency [24]. For instance, as demonstrated by Figueiredo-Barros et al. [25], the activity of Polychaeta (specifically *Heteromastus similes*, a conveyor-belt deposit feeding worm) in surface sediment layers can enhance CH_4 flux through the sediment–water interface by up to 3.7 times.

Gas bubble formation in sediments occurs only when the sum of the partial pressures of all dissolved gases exceeds the total ambient pressure within the sediments [23,26,27]. This ambient pressure is the sum of atmospheric pressure at the lake surface (~1 bar) and the hydrostatic pressure of the water column at a certain depth. Consequently, gas bubble formation is generally confined to relatively shallow areas of water bodies. In contrast, methane release from sediments in deep lake zones primarily occurs through diffusion [28]. Strayer et al. (1978) [29] highlighted that those human-induced changes to the source, rate, and pathways of CH_4 production are contributing to a net increase in emissions from estuaries.

Shallow lakes are believed to be among the most significant sources of methane production on a global scale [18,30]. Bastviken et al. [18] found out that methane emissions from lakes can be estimated from such characteristics as lake area, water depth, the anoxic

volume fraction of the lake, concentrations of total phosphorus, methane, and dissolved organic carbon in water. Using the expressions of dependencies of these parameters, the paper presents estimates of the global methane emission from open reservoirs. According to Bastviken et al. [18], methane emission in shallow lakes is due to ebullition prevails, while the maximum ebullition probability falls on the depth interval of 0.5–1 m. Thus, Schmiedeskamp et al. [30] found that methane emissions from Lakes Windsborn (western Germany) (maximum depth ~1.7 m) and Heideweiher (northwest of Germany) (maximum depth ~0.83 m) were mainly by ebullition. The average methane fluxes in the lakes were estimated at 3.5 and 12.2 mmol/(m^2·d), respectively.

Zhu et al. [10] also reported significant methane fluxes due to ebullition in the shallow (less than 1 m depth) Medo Lake (Tibetan Plateau) during the summer months of 32.45 mg/(m^2 h),which accounted for 93% of the total methane flux (diffusion plus ebullition) into the atmosphere. Unfortunately, the vertical profile of sediment density and the presence of the surface layer of elevated density formed due to the highest photosynthetic green algae activity were not indicated in the work. Shallow water bodies are characterized by high activity of photosynthesis and a calcite coating of sediment particles, which preserves organic matter and limits the production of methane.

The aim of our present study was to evaluate the gas ebullition fluxes on the shallow terrace of the bottom of the Lake Juodis, where areas of abundant carbonate deposits were found [31], and compare them to those in the dominant domain with black silt sediments. According to Meysmany et al. [32], bioturbation (subdiffusion) in the carbonate sediments is minimized due to difficulties for benthic organisms to obtain nutrition when sediment particles are covered by calcite. It creates an opportunity to study the impact of the ebullition processes on physical mixing of the lake bottom sediments, as other mixing processes are suppressed. Deposited radiocesium ^{137}Cs from the atmosphere settles onto the surface of bottom sediments in layers, forming an archived vertical profile [31], therefore examination of its activity distribution shape can be informative for analysis of sediments' vertical mixing. We have measured the ^{137}Cs activity concentration profile of the Lake Juodis sediment layers and confirmed a low mixing phenomenon attributable to calcite-enriched sediments.

Comprehensive studies on ebullition processes in similar shallow lakes were performed by Zhu et al. [10] and Schmiedeskamp et al. [30]; however, information on the vertical profiles of sediment density as well the impact of carbonates (calcite) in the works were not considered. Our study aimed to fill the gap and was motivated by increased public interest in the issues related to the greenhouse gas emissions from lake ecosystems in connection with climate warming. It reveals that such factors as abundance of carbonates in the sediments may significantly reduce biogas ebullition fluxes.

2. Materials and Methods

2.1. Object of the Ebullition Flux Study

A study conducted on the processes influencing gas ebullition fluxes from sediments was in the northern shallow bottom terrace (depth ~1.0–1.6 m) of Lake Juodis (54°46′49″ N, 25°26′29″ E). This lake, having areas with distinct types (carbonate and black silt) of sediments, is located near Vilnius (17 km to northeast). It is a flowing shallow lake within a chain of lakes (Figure 1) with sapropelic sediments, rich in organic matter. The lake is subject to natural eutrophication processes, lacks groundwater springs, has no significant artificial contamination or nutrition sources, and has extensive wetlands on the banks. Pine forest growing on the banks protects the lake from winds. The glacial origin basin (groove type) of the lake has two parts: the northern part is a shallow terrace with depth of ~1.6 m, while the southern part is wider, and its depth reaches ~3.5 m. The lake area is 0.1 km^2, the drainage basin area reaches ~3.5 km^2, and the hydraulic retention time is ~0.3 y. The content of organic matter in sediments was estimated to be very high (~68%), while the typical dry matter amount in the surface layer of sapropelic type sediments ranges within 23–30 g/L [33]. The thickness of the sediment layer in the northern shallow part of the lake

was evaluated to be about 5–7 m [34]. The mineral content of the surface water is maximal in winter (~174 mg/L). At the bottom terrace, two permanent stations were created in 2003 (Figure 1) to examine an annual course of standard water and sediment liquid parameters.

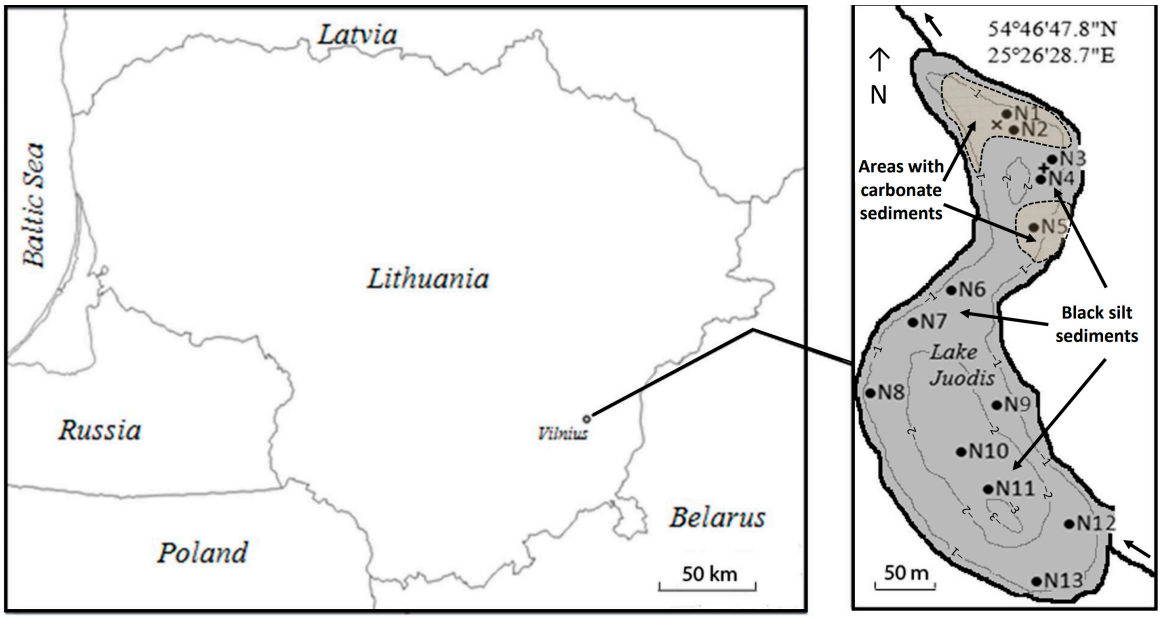

Figure 1. Scheme of the biogas (methane) sampling sites (N1–N13) (•) using the "Jellyfish" apparatus on 8 August 2003 in Lake Juodis and the location of the northern (×) and southern stations (+) on a shallow bottom terrace. Carbonate sediment N1 and N2 (•) were sampled near the northern station (×); black silt sediment N3 (•) was sampled near the southern station (+); inflow and outflow of the brook (←).

Two pairs of passive collectors (ordinary glasses placed upside-down and filled with water, area ~37.4 cm^2) were hung at every station at the ~1 m distances from the station holders. The collectors were exposed from 13–88 (warm season) to 220 days (cold season). The sequence of gas accumulation in passive collectors was monitored visually during the warm season when visiting the northern platform 1–2 times a week. During long exposures of passive collectors, methane can be oxidized to carbon dioxide.

A northern station (×) (water depth ~100–110 cm) was located in the region of carbonate deposits, which were formed due to the photosynthesis of the sediment green algae. This part of the terrace was always saturated with oxygen in winter [33]. A southern station (+) (depth ~150 cm) was located in the area with black silt sediments where in the winter period anaerobic conditions were created.

In 2000, our studies began in connection with the climate change investigations on the biogas ebullition, thermodynamic regime, and self-cleaning processes of Lake Juodis. The factors having an impact on the biogas releases to the atmosphere were examined.

2.2. Parametrization

Standard water and sediment parameters (pH, temperature, oxygen concentration, and conductivity) have been periodically measured at the stations since February 2003. Measurements in the northern part of the lake were conducted using a portable HAND MULTILAB 12 device (SCHOTT) with a 3-meter-long cable. Year-round measurements of standard water parameters in the lake were previously reported in our earlier works, which aimed to study the lake's thermodynamics and clarify the reasons for elevated bottom water temperatures in winter [35].

2.3. Sample Collection and Analysis

An Ekman–Birge type sampler (an improved version, ~40 cm height) was used to collect sediment cores for studying the vertical profile of ^{137}Cs radionuclide contamination. The sampler consisted of a steel tube with a square cross-section (14 × 14 cm) and a manually operated spring-loaded bottom shutter. Sampling was performed with weight compensation, and an additional float was used to control the depth to which the sampler penetrated the sediments. The sediment cores were sliced into 2–2.5 cm-thick horizontal layers and placed in plastic containers. The samples were allowed to settle, and sediment volumes were recorded. The samples were dried at room temperature. Their weights were measured using VLV-100 scales under thermostatic conditions (at a temperature range of 40–50 °C) until a constant weight was achieved.

The activity of ^{137}Cs in sediment samples was measured using a CANBERRA gamma-spectrometric system equipped with an HPGe detector, which has a 26.2% relative efficiency and a resolution ~1.76 keV at 1.33 MeV on the 661.62 keV gamma line (^{137m}Ba, a daughter product of ^{137}Cs). Measurements were conducted in standard geometry, calibrated for known efficiencies based on the sample densities. Measurement errors were calculated using the GENIE-2000 software, with standard deviations not exceeding 5% for active samples and 15% for less active sediment layers. No activity corrections were made for the sampling date, as the measurements were conducted shortly after sampling.

X-Ray diffraction (XRD) patterns of the composite consisting of black silt and carbonate sediments were measured using a SmartLab (Rigaku, Akishima, Japan) device equipped with an X-ray tube with a 9 kW rotating Cu anode. The measurements were conducted in Bragg–Brentano geometry, with a graphite monochromator on the diffracted beam using step scan mode with a step size of 0.02° (in 2θ scale) and a counting time of 1 s per step. The 2θ range for the measurements was 5–75°. Phase identification was carried out using the PDXL-2 software package (Rigaku) and the ICDD Powder Diffraction Database PDF4+ (2023 release). Mineral content was estimated using the Reference Intensity Ratio (RIR) method.

Biogas samples were released into a vacuum chamber and preconditioned with a desiccant to remove moisture from the samples. The main components of the biogas were characterized using infrared absorption spectrometry. The IR4-CO_2 instrument, manufactured by Deksna Ltd., was operated in the mid-infrared range. Specific IR wavelength values in the absorption spectra were assigned to the target gases: CH_4 at 3.30 μm (3030 cm^{-1}), CO_2 at 4.26 μm (2347 cm^{-1}), CO at 4.64 μm (2155 cm^{-1}). The reference signal wavelength was fixed at 3.91 μm (2558 cm^{-1}). The instrument sensors were calibrated using pure CH_4 gas (quality 4.5) and a calibration gas mixture containing CO (3.5%), CO_2 (14.0%), and C_3H_8 (2000 ppm) in N_2. During calibration, all gases were diluted with N_2 as the carrier gas.

2.4. Supplementary Results

2.4.1. Sediment Characterization

Microscopic photographs of the black silt and carbonate sediment samples are presented in Figure 2a,b, respectively. The black silt sediments (Figure 2a) show an abundance of decomposing organic matter of plant origin and trapped biogas bubbles. Meanwhile, the carbonate sediments (Figure 2b) also reveal the presence of green algae.

We also determined that radioactive pollution by ^{137}Cs in the lake was caused by the fallout of nuclear weapons testing and the Chernobyl accident. This allowed us to use radiocesium in the bottom sediment layers as a tracer to examine the physical mixing processes of the sediments and to identify whether the bottom sediment layers were undisturbed.

XRD data indicate that the mineralogical composition of the sediment samples varies. The analysis revealed that the black silt sediments are primarily composed of crystalline quartz (ICDD #00-046-1045)—accounting for approximately 52 wt.%. Additionally, the sediments contain pyrite (ICDD #00-042-1340)—19.4 wt.%, a tectosilicate microcline (ICDD

01-070-6187)—20.7 wt.%, and the clay mineral muscovite (ICDD # 01-087-0691) at about 8 wt.%). There may also be an amorphous phase comprising approximately 20–30 wt.%.

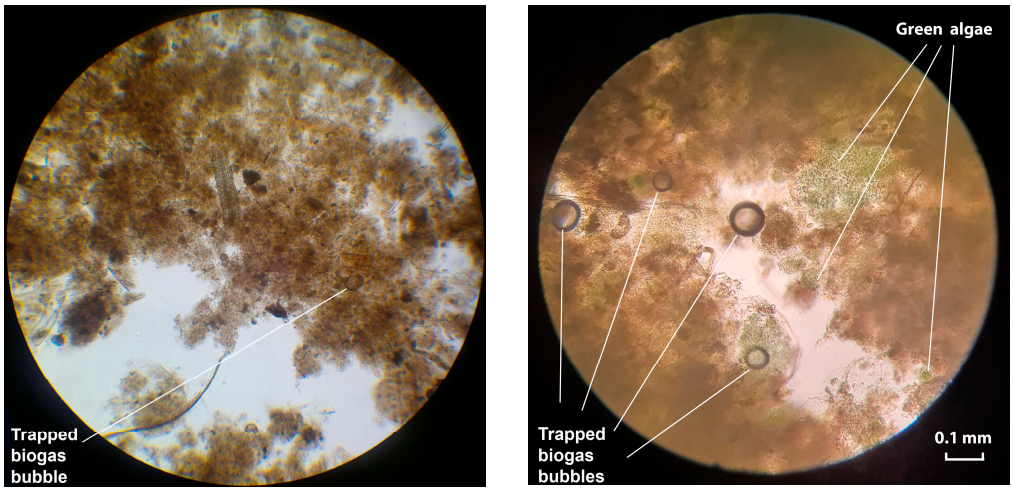

(**a**) (**b**)

Figure 2. Microscopic photographs of the extracted sediment samples: (**a**) black silt, typically containing a large amount of decomposing organic matter and trapped biogas bubbles; (**b**) carbonate sediments, containing remnants of green algae.

The mineral composition of the carbonate sediments is as follows: calcite ($CaCO_3$) (ICDD # 01-083-4601), which predominates at approximately 82 wt.%, along with small amounts of quartz (12 wt.%) and pyrite (4 wt.%).

2.4.2. Oxygen Production on the Sediment Surface Due to the Photosynthetic Activity of Green Algae

Data on the standard parameters and the distribution of radiocesium carbonate and black silt sediments were obtained [33]. Observations have shown that during the warm season, the entire surface of the terrace is covered with green algae, whose life cycle influences sedimentation in this lake (~0.5–0.6 cm/y). In winter, anaerobic conditions typically form at a depth of ~120 cm. Thus, the shallow northern part of the terrace remains in the aerobic zone year-round [36]. Due to the photosynthetic activity of green algae on the surface of carbonate deposits, the water column is constantly enriched with oxygen (Figure 3a,b). This process begins in spring, when the increased transparency of the ice promotes oxygen production at the sediment surface (Figure 3c) facilitating the formation of a calcite coating on the surface of sediment particles. Green algae also produce oxygen through photosynthesis during the warm season in the black silt zone (Figure 4a,b). At the same time, a calcite coating forms on the surface of the black silt sediment particles, but it dissolves under anaerobic conditions during the winter.

However, it should be emphasized that the gradual decrease in oxygen concentration with sediment depth is illusory. Oxygen sensors are designed for use in water only. When such a sensor is inserted into the sediments, a vertical channel is created through which bottom water, which still contains significant oxygen concentrations, enters the sediment layers. It distorts the actual profile, which is expected to show a sharp cutoff at the surface. As a result, relatively high oxygen concentrations are still measured at sediment depths of up to 15–20 cm.

2.4.3. Vertical Profiles of ^{137}Cs Activity Concentrations and Sediment Density in Samples of the Shallow Bottom Terrace

In the zone of carbonate sediments, two sediment samples were collected on 16 July 2003: one at a depth of 110 cm (Figure 5) and another at a depth of 120 cm (Figure 6). Due to the high lime content, the carbonate sediments turn into a white powder when dried. In

the first sample (Figure 5b), the calcite coating on the sediment particles caused the density to reach a maximum of 50 g/L at a depth of 6 cm. The weight fraction of calcite at a depth of 14 cm was up to 45%. A layer of increased density resulting from the presence of calcite extended to a depth of 20 cm. Below this layer, the sediments acquired a gel-like structure due to abundance of organic matter. In the second sample (Figure 6b), calcite deposits were present down to a depth of 15 cm, with a maximum density of ~42 g/L.

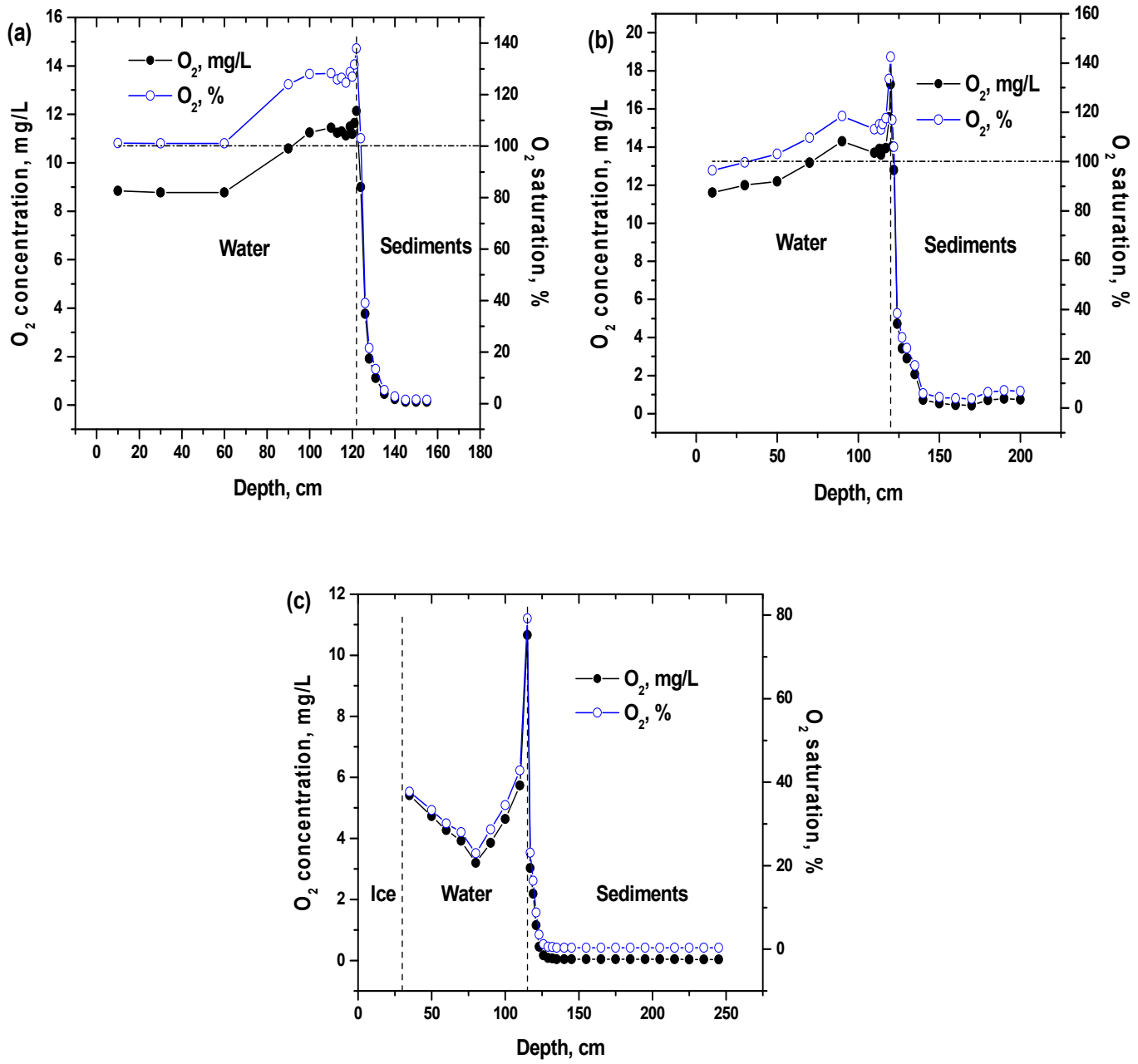

Figure 3. Vertical profiles of oxygen concentrations (mg/L) in the northern part of the lake in the green algae area (northern station) on 19 August 2003 (**a**) (bottom depth~122 cm), 3 November 2003 (**b**) (bottom depth~120 cm), and 16 March 2004 (**c**) (bottom depth~115 cm, the transparent ice thickness of ~32 cm).

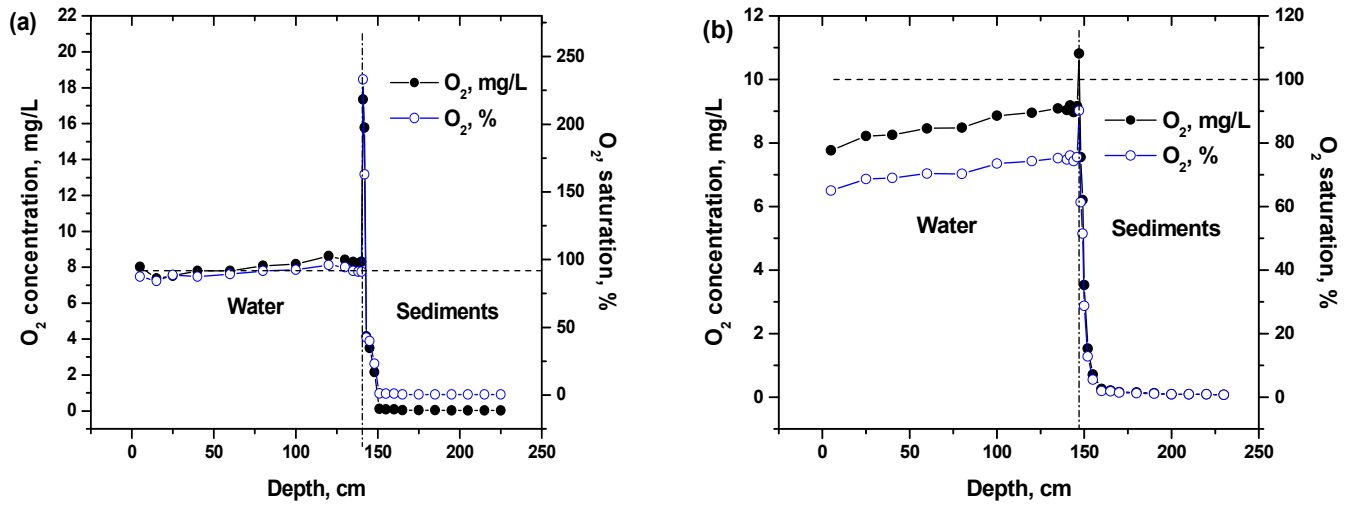

Figure 4. Vertical profile of oxygen concentrations (mg/L) in the northern part of the lake in the area of black silt sediments (southern station) on 11 August 2004 (**a**) (bottom depth~141 cm) and 13 October 2004 (**b**) (bottom depth~147 cm).

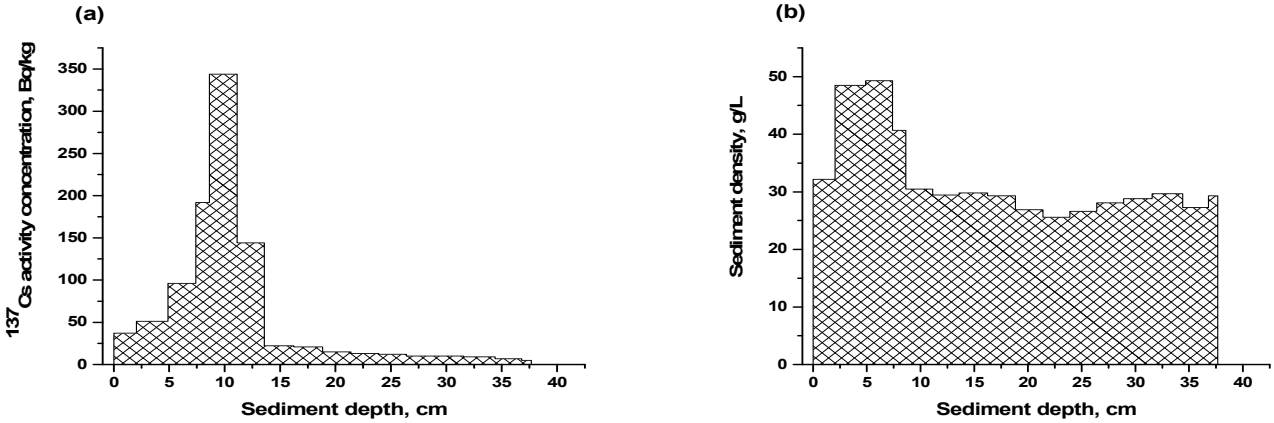

Figure 5. Vertical profiles of ^{137}Cs activity concentration (**a**) and sediment density (**b**) in sample N1 of bottom sediments (rich in carbonate deposits) collected on 16 July 2003 near the northern sampling station (×) at a depth of 110 cm.

The sediment sample in the area of black silts (southern station) was taken on 29 October 2003 at a depth of 140 cm (Figure 7a,b). Unlike carbonate sediments, black silt sediments in dry form are black. Due to the absence of a calcite coating on the granules of black silt sediments in the upper layers of the vertical density profile of these sediments, no characteristic peak in the density profile of carbonate sediments was observed (Figure 7b). The vertical profile of ^{137}Cs activity concentration (Bq/kg) in this sample (Figure 7a) has a flatter slope below the maximum of the ^{137}Cs activity concentration, and in the section of the same profile above this maximum, which is more convex. This profile (black silt) also differs significantly from those taken near the northern station (carbonate-enriched), where more sharp peaks of ^{137}Cs activity concentrations (Bq/kg) are present in the vertical profiles (Figures 5a and 6a).

It was determined that the calcite deposits in the lake act as a specific barrier to the migration of ^{137}Cs. The calcite coating on sediment particles prevents the backward flux of ^{137}Cs into the bottom water transforming the respective bottom areas into a radionuclide sink. Calcite preserves the shape of the primary ^{137}Cs vertical profiles, which were formed by free-ion diffusion shortly after the deposition event [31,35]. This also confirms that the sediment layers were not physically mixed either by biogas ebullition processes or by bioturbation.

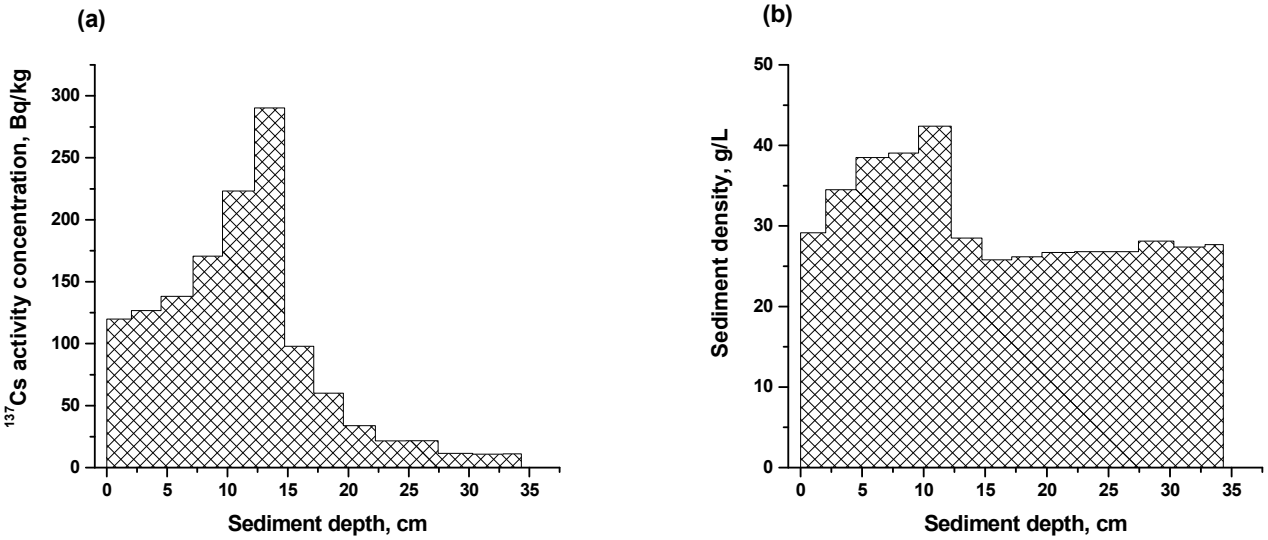

Figure 6. Vertical profiles of ^{137}Cs activity concentration (**a**) and sediment density (**b**) in the sample N2 of bottom sediments (rich in carbonate deposits) collected on 16 July 2003 near the northern sampling station (×) at a depth of 120 cm.

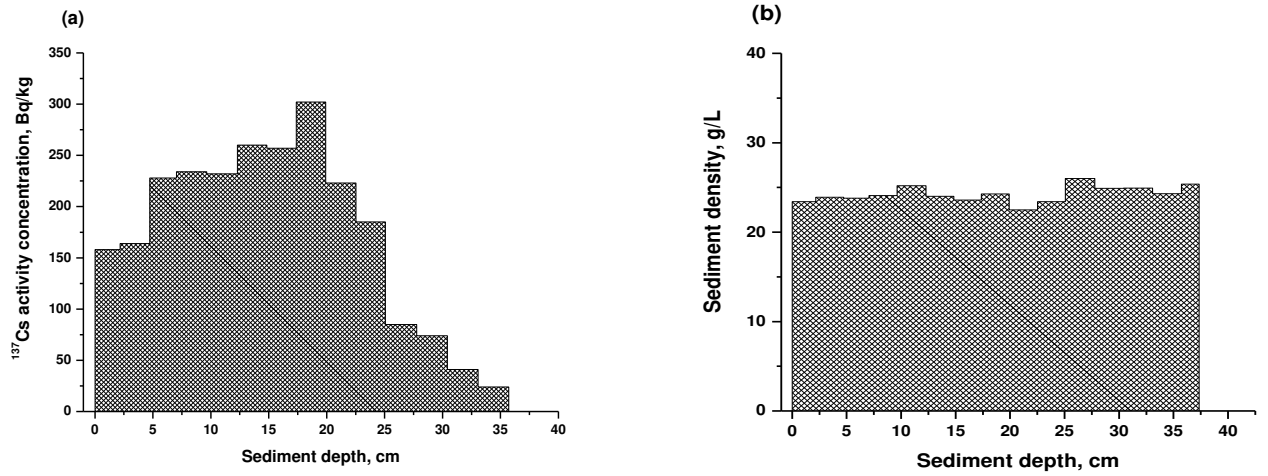

Figure 7. Vertical profiles of ^{137}Cs activity concentration (**a**) and sediment density (**b**) in the sample of black silt deposits (N3) taken on 29 August 2003 near the southern sampling station (+) at a depth of 140 cm.

3. Results of the Ebullition Flux Measurements

3.1. Preliminary Studies of Biogas Ebullition Intensities from Lake Sediments Using the "Jellyfish" Apparatus

Preliminary studies of biogas ebullition intensities in various zones of the lake were conducted in August 2003 using a self-made device (referred to as the "Jellyfish") for biogas collection. However, the composition of the biogas was additionally collected and analyzed at the end of the warm season in 2024. Analysis of the collected gas using an IR4-CO_2 device revealed that it consisted of CH_4—58.5 ± 1.9% and CO_2—1.5 ± 0.1% with no detectable CO. The remaining 40 ± 1.9% was attributed primarily to N_2 with traces of O_2. The most plausible explanation for the high CH_4 content in Lake Juodis, along with elevated CO_2 emissions, is anaerobic decomposition of organic matter beneath the silt layer.

A map of the biogas sampling sites (N1–N13) (●) in Lake Juodis using the "Jellyfish" apparatus is shown in Figure 1. The "Jellyfish" device consists of a glass dome with a metal cross located inside, on which eight metal rods, each 55 cm long and 6 mm in diameter, are mounted. A measuring tube with a valve is located at the top of the dome. Before use, the

device was filled with water and lowered to the bottom using a cable. The depth of the rods' immersion into sediments could be adjusted with the help of an additional float.

When examining the full depth of rod immersion (~40 cm) at various points on the northern shallow-water platform of the lake (carbonate deposits), the volume of released biogas ranged from 2 to 5 mL; however, in the southern part of the lake (black silt), the volume ranged from 4.3 to 60 mL (Table 1). Near the southern station, at points N3 and N4, the biogas volume was double that of the northern station, reaching 5 mL (Table 1). In the isthmus region and the southeastern side of the southern part of the lake, maximum volumes of 10 and 60 mL were recorded. This substantial biogas release may be attributed to a layer of rapidly decomposing organic matter beneath the silt layer in these parts of the lake. The temperature of the surface of the sediments during the measurements varied in the range of 21.6–23.7 °C. Measurements were conducted during the daytime, starting at 8:30 A.M.

Table 1. Results of biogas sampling conducted on 8 August 2003 using the self-made "Jellyfish" apparatus with a rods immersion depth of ~40 cm into the surface sediments.

Sampling Site	Depth, m	Sediment Type	Temperature of the Water Surface, °C	Temperature of the Sediment Surface, °C	Biogas Volume, mL
N1	1.0	Carbonate	21.3	21.6	2.0
N2	1.1	Carbonate	21.5	21.8	3.0
N3	1.6	Black silt	22.0	22.0	5.0
N4	1.55	Black silt	22.0	22.0	5.0
N5	1.3	Carbonate	22.4	22.8	3.5
N6	1.4	Black silt	22.6	22.8	5.5
N7	1.3	Black silt	22.8	22.8	10
N8	1.8	Black silt	23.0	23.7	10
N9	1.3	Black silt	23.0	23.2	20
N10	2.5	Black silt	23.1	23.4	4.8
N11	2.9	Black silt	23.1	23.4	4.3
N12	1.4	Black silt	23.2	23.5	60.0
N13	1.6	Black silt	22.9	23.2	4.5

3.2. Study of Biogas Ebullition Intensities from Lake Sediments Using Passive Biogas Collectors

Typically, after long-term exposure, gas samples were collected simultaneously at both stations from both collectors. The data from the collectors (individual glass containers) at the same station showed slight variations differing by 10–15%. The amount of gas in each collector during exposure is primarily proportional to the average gas ebullition flux generated by sediments beneath the collector's area, as well as the probability of a vertical gas channel forming in that area. It is assumed that after prolonged exposures lasting several weeks, this probability approaches unity. The measured gas ebullition fluxes at the northern station from 18 September 2005 to 19 May 2007 and from 8 October 2008 to 6 October 2010 are shown in Figure 8a,b. Similarly, the data for gas ebullition fluxes at the southern station from 18 September 2005 to 6 August 2007 and from 8 October 2008 to 19 October 2010 are presented in Figure 9a,b.

Based on the measurement data at the northern station (Figure 8a), the annual gas ebullition flux in the area of carbonate sediments was estimated at 21.9 L/(m^2·y) from 13 November 2005 to 13 November 2006. During the second series of measurements, from 8 October 2008 to 8 October 2009 (Figure 8b), this flux increased to 23.0 L/(m^2·y). However, between 2009–2010 from 19 October 2009 and 19 October 2010, it decreased to 16.9 L/(m^2·y) (Figure 8b). These values are of the same order and are characteristic of the northern station.

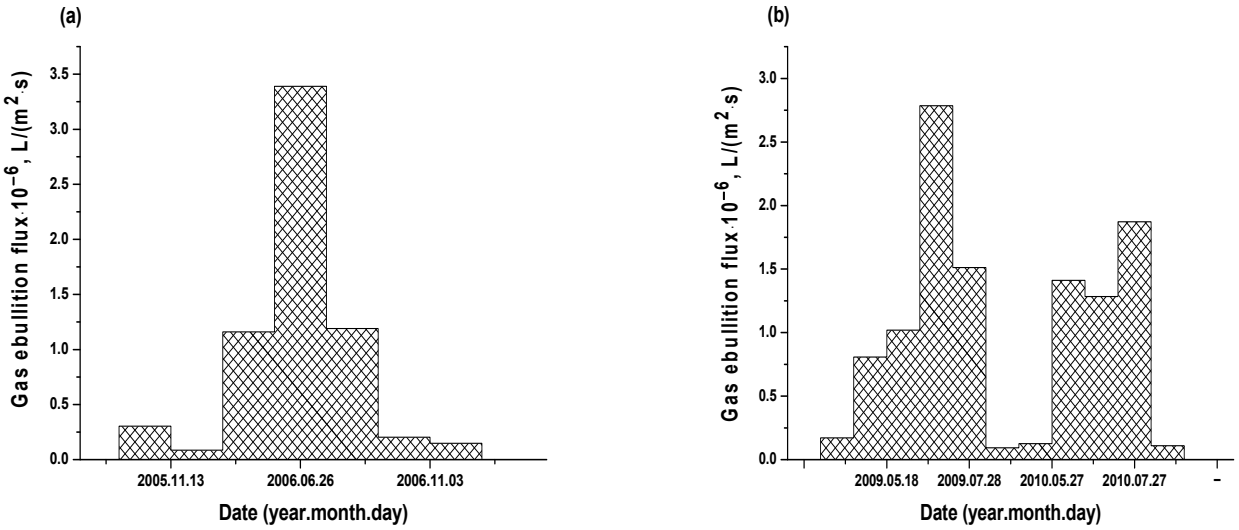

Figure 8. Biogas ebullition flux (L/m^2·s) from 18 September 2005 to 19 May 2007 (**a**) and from 8 October 2008 to 6 October 2010 (**b**) at the northern station (carbonate sediments).

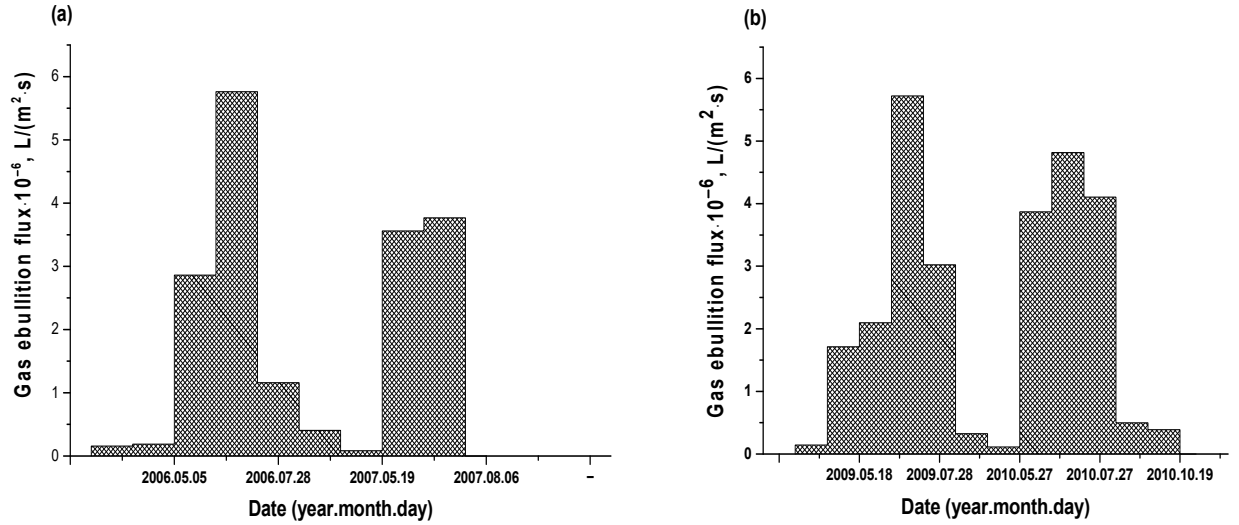

Figure 9. Biogas ebullition flux (L/m^2·s) from 18 September 2005 to 6 August 2007 (**a**) and from 8 October 2008 to 19 October 2010 (**b**) at the southern station (black silt sediments).

According to the measurement data at the southern station (Figure 9a) the annual biogas ebullition flux in the area of black silt sediments was estimated at 38.5 L/(m^2·y) from 13 November 2005 to 13 November 2006. During the second series of measurements from 8 October 2008 to 8 October 2009 (Figure 9b), this flux increased to 43.2 L/(m^2·y). Between 9 October 2009 and 19 October 2010, it decreased slightly to 41.6 L/(m^2·y) (Figure 9b). These values are of the same order and are characteristic of the southern station.

Ebullition fluxes exhibit a periodic pattern, peaking during the warm season when the decomposition of organic matter is most active due to the elevated temperatures of surface sediments.

Estimates indicate that the annual gas ebullition flux at the southern station is nearly twice as large as at the northern station. This suggests that the calcite coating on the surface of sediment particles partially preserves the organic matter of the particles. In winter (February), the surface temperatures of carbonate sediments were typically ~2 °C. Meanwhile, the surface temperature of black silt sediments at the deeper site of southern station was ~4.3 °C. In the deepest part of the lake (southern side), surface sediment temperatures consistently exceeded 5 °C during this period. Large gas bubbles were often visible under the ice in the southern part of the lake during winter, a phenomenon less

frequently observed in the northern part. This implies that in winter, gas ebullition flux in the southern part of the lake is significantly higher than in northern part.

In the mid-summer, when the sediment surface temperature reaches its peak, it is ~0.2–0.3 °C lower than the surface water temperature near the northern station and about ~0.3–0.5 °C lower near the southern station. At the deeper southern station, where the sediments are more distant from the surface of the lake water, the temperature difference between the surface water and the sediment surface can reach ~3 °C. The temperatures in Table 1 reflect conditions in early August 2003, when the Lake Juodis region experienced slightly cooler air masses than usual, resulting in a less pronounced temperature difference.

4. Discussion

Our study revealed that during the exposure periods of passive collectors in 2005–2010, the annual biogas ebullition fluxes from sediments at the northern station (carbonate sediments) and the southern station (black silt deposits) stations varied within the range of 16.9–23.0 L/(m^2·y) and 38.5–43.2 L/(m^2·y), respectively. This indicates that the biogas ebullition fluxes from carbonate sediments were nearly half those from black silt sediments. This also supports the fact that the calcite coating on the particles of carbonate sediments partially preserves the organic matter of the sediments. The measured vertical profiles of oxygen concentration in the carbonate barrier zone indicate that this area becomes a major source of oxygen for the overlying water and sediments, due to the photosynthetic activity of green algae growing there. The oxygen also helps to preserve carbonates in the sediments from dissolution. Oxic conditions can prevent dissolution of carbonates in certain layers of sediment. For example, under anoxic conditions, microbial processes can generate acids (like H_2S), which may dissolve carbonates. Oxygen limits the accumulation of such acids, preserving carbonate minerals. Therefore, the decrease in the annual biogas ebullition biogas flux from the carbonate sediments zone can primarily be linked to a reduction in the thickness of the active sediment layer in which methane bubbles can form. Additionally, it should be noted that generated methane can be oxidized at the sediments' surface, leading to the partial dissolution of the produced carbon dioxide in the water.

The specific shape of the vertical profiles of ^{137}Cs activity (Bq/kg and Bq/L) observed in carbonate sediments shows a complete absence of ^{137}Cs migration and reflects the archival record of atmospheric radioactive fallout. The profiles maintain their shapes over time and can be used for dating of radioactive fallout. The constancy in the vertical profiles of ^{137}Cs activity concentrations in carbonate sediments indicates the absence of mixing due to gas ebullition fluxes. The low buoyancy forces (Archimedes principle) acting on small deep-formed methane bubbles in the sediments are insufficient to overcome the viscosity of the sediments and cause mixing. As these bubbles increase in size, they obtain a flattened disk shape and can move upward by displacing sediment particles, thus forming a vertical channel to the surface.

Vertical profiles of sediment density from samples collected in the carbonate zone of the shallow bottom terrace at depths of 110 and 120 cm show that the carbonate coating on sediment particles disappears at depths of 20 and 15 cm, respectively. This indicates that active bacteriological decomposition of organic material can only occur starting at these sediment depths. This situation is similar to that in wetlands and rice fields, as described in [37]. As was demonstrated in that study, the capillary structure of plant stems and roots allows oxygen to reach significant depths of the active soil layer or sediments in rice fields, where methane is produced. With a sufficient density of plant roots per unit area, sufficiently large oxidation of methane can undergo significant oxidation at these depths, preventing the formation of bubbles. In such a case, remaining methane can only enter the atmosphere by diffusion. Thus, in wetlands and rice fields, plants act as regulators of the balance between diffusive and ebullitive methane fluxes into the atmosphere, limiting the thickness of the active layer in which methane bubbles can form. Similarly, carbonate sediments in Lake Juodis perform a restrictive function, reducing the thickness of the active

layer, in which methane bubbles can form. As a result, this leads to a decrease in the ebullition flux of methane.

Our results (recalculated to pure biomethane 22.5–25.3 L/(m^2·y)) of the averaged annual ebullition biogas fluxes from black silt sediments are in a good agreement with the data from [38] (~29.1 L/(m^2·y)) in the tidal zone of the White Oak River estuary and approximately four times as low as the data from Casper et al. [39] (~98.1 L/(m^2·y)) for Lake Priest Pot, UK. This discrepancy is likely due to the higher temperature regime in that water body. According to [6], in Lake Vohlen (Switzerland), the average annual methane flux from ebullition alone was estimated at ~86 mg/(m^2·d) (~44 L/(m^2·y)), which also aligns quite well with our results for the black silt sediment zone. Also, our data on the annual gas emission fluxes are consistent with the data of annual methane fluxes data (where ebullition dominates) from Lakes Windsborn and Heideweiher [38], which were 28.6 and 99.7 L/(m^2·y), respectively, for 2017–2018. Moreover, the higher methane flux in the latter case is due to Lake Heideweiher partially drying up during the summer months. This leads to a sharp increase in methane emissions when the water level in the lake falls. In the tropical Brazilian Pantanal region, in Lakes Medalha and Mirante, the measurements from 2004–2005 showed average methane ebullition fluxes of 75.7 and 41.9 L/(m^2·y), respectively (~90% of the total flux to the atmosphere). These obtained higher values for tropical wetlands are in reasonable agreement with our results gained in the shallow platform of temperate Lake Juodis, if one takes into account the impact of the temperature. This variation phenomenon is proved also by the observed influence of the climate zone and seasonality on the biomethane flux from the other lakes (see Table 2).

Table 2. Comparison of the seasonal biomethane ebullition rates from lakes in different climate zones.

Study Area	Country	Year of Analysis	Month of Analysis	CH_4 Emission, L/(m^2·y)	Reference
Temperate Lake Juodis carbonate sediments	Lithuania	2008–2009	October–April	3.4 *	This study
		2009	June–July	36 *	
Temperate Lake Juodis black silt sediments		2008–2009	October–April	2.9 *	
		2009	June–July	72 *	
Subtropical Lake Donghu	China	2003	March–May	4.4	[21]
			June–August	36.4	
			Sepember–November	7.8	
Boreal Lake Erssjön	Sweden	2012–2013	April	6.5	[40]
Boreal Lake Följesjön in transformation to a wetland			July	14.5	
Boreal Lake Skottenesjön			October	2.8	

Note: * Recalculated to pure CH_4 from monthly measured total biogas flux by assuming 58.5% contribution from biomethane.

In our study, monthly biogas emissions during the warm season (36–72 L/(m^2·y)) are higher than in most temperate or northern region lakes (e.g., Sweden) and can even exceed those of the subtropical region (e.g., China). This indicates that in temperate regions, biogas emissions depend on seasonality, the amount of organic matter, and the level of eutrophication. In tropical regions, biogas emissions are primarily driven by temperature and precipitation, resulting in emissions that can be extremely high or very low. In temperate and northern regions, temperature and freezing conditions significantly influence seasonal fluctuations in biogas emissions. Thus, in general, Lithuania falls into an

intermediate biogas emission zone, reflecting the impact of seasonality and organic load, with intensities lower than those in tropical regions but higher than in northern areas.

Also, the data obtained in our work indicate that when assessing methane emission from water bodies, it is crucial to examine the characteristics of bottom sediments and the vertical profiles in the shallow parts of water bodies. In shallow waters, photosynthetic activity of the green algae contributes to the formation of carbonate sediments in which organic matter is preserved, thus significantly reducing methane emissions.

5. Conclusions

The calcite coating on the surface of sediment particles, resulting from the photosynthetic activity of green algae in the carbonate barrier zone, helps preserve organic matter and reduce biomethane production. The methane ebullition fluxes in areas with carbonate deposits are several times lower than those from black silt sediments, as the bacteriological decomposition of organic matter and intensive methane production in sediments with carbonate coating occurs only at depths where the calcite coating on sediment particles disappears. Carbonate sediments reduce the thickness of the active layer in sediment where intensive formation of biomethane bubbles formation is possible. Also, biogas emissions very much depend on seasonality.

The preserved ^{137}Cs activity concentration peaks in the vertical profiles of carbonate sediments indicate absence of ^{137}Cs migration. This constancy demonstrates the lack of sediment mixing due to percolating ebullition gas fluxes.

The results of our investigation indicate that when studying biomethane ebullition fluxes from shallow lakes, it is necessary to conduct a preliminary operational analysis of the qualitative factors of bottom sediments, including their composition (e.g., presence of calcite), as well as vertical density profiles. These factors (specific to the bottom sediments organics, mineral additives, and environmental conditions) can significantly affect the ability of bottom sediments to produce biomethane and influence its release flux into the atmosphere through ebullition and deserve more systematic examination.

Author Contributions: Conceptualization, E.M. and N.T.; Formal analysis, E.M., L.K.-J., Z.Ž. and M.K.; Investigation, E.M. and N.T.; Data curation, Z.Ž., N.P. and V.D.; Writing—original draft, E.M. and N.T.; Writing—review & editing, E.M., L.K.-J., M.K., V.D. and N.T. All authors have read and agreed to the published version of the manuscript.

Funding: This research received no external funding. The authors received their routine salary from their host scientific research institutions.

Data Availability Statement: All data is provided in the manuscript, no external datasets are available.

Acknowledgments: The authors express their deep gratitude to Eva Koviazina and Anastasija Moisejenkova for their help in field expeditions. The authors thank Vidas Pakštas for XRD analysis as well Jonas Didžbalis and Žilvinas Ežerinskis for fruitful assistance in biogas composition measurements.

Conflicts of Interest: The authors declare no conflict of interest.

References

1. World Health Organization. Climate Change. 2023. Available online: https://www.who.int/health-topics/climate-change#tab=tab_1 (accessed on 9 June 2024).
2. IPCC. Emissions Trends and Drivers. In *Climate Change 2022: Mitigation of Climate Change. Contribution of Working Group III to the Sixth Assessment Report of the Intergovernmental Panel on Climate Change*; Cambridge University Press: Cambridge, UK; New York, NY, USA, 2022. [CrossRef]
3. Saunois, M.; Stavert, A.R.; Poulter, B.; Bousquet, P.; Canadell, J.G.; Jackson, R.B.; Raymond, P.A.; Dlugokencky, E.J.; Houweling, S.; Patra, P.K.; et al. The Global Methane Budget 2000–2017. Earth Syst. *Sci. Data* **2020**, *12*, 1561–1623. [CrossRef]
4. Striegl, R.G.; Michmerhuizen, C.M. Hydrologic influence on methane and carbon dioxide dynamics at two north-central Minnesota lakes. *Limnol. Oceanogr.* **1998**, *43*, 1519–1529. [CrossRef]
5. Bastviken, D.; Tranvik, L.J.; Downing, J.A.; Crill, P.M.; Enrich-Prast, A. Freshwater Methane Emissions Offset the Continental Carbon Sink. *Science* **2011**, *331*, 50. [CrossRef]

6. DelSontro, T.; McGinnis, D.F.; Sobek, S.; Ostrovsky, I.; Wehrli, B. Extreme methane emissions from a Swiss hydropower reservoir: Contribution from bubbling sediments. *Environ. Sci. Technol.* **2010**, *44*, 2419–2425. [CrossRef]
7. Sanches, L.F.; Guenet, B.; Marinho, C.C.; Barros, N.; de Assis Esteves, F. Global regulation of methane emission from natural lakes. *Sci. Rep.* **2019**, *9*, 255. [CrossRef] [PubMed]
8. Santoso, A.B.; Hamilton, D.P.; Schipper, L.A.; Ostrovsky, I.S.; Hendy, C.H. High contribution of methane in greenhouse emissions from eutrophyc lake: A mass balance synthesis. *N. Z. J. Marin. Freshw. Res.* **2021**, *55*, 411–430. [CrossRef]
9. Sun, H.; Lu, X.; Yu, R.; Yang, J.; Liu, X.; Cao, Z.; Zhang, Z.; Li, M.; Geng, Y. Eutrophication decreased CO_2 but increased CH4 emissions from lake: A case study of a shallow Lake Ulansuhai. *Water Res.* **2021**, *201*, 117363. [CrossRef]
10. Zhu, D.; Wu, Y.; Chen, H.; He, Y.; Wu, N. Intense methane ebullition from open water area of a shallow peatland lake on the eastern Tibetan Plateau. *Sci. Total Environ.* **2016**, *542 Pt A*, 57–64. [CrossRef]
11. Balmer, M.B.; Downing, J.A. Carbon dioxide concentrations in eutrophic lakes: Undersaturation implies atmospheric uptake. *Inland Waters* **2011**, *1*, 125–132. [CrossRef]
12. Pacheco, F.S.; Roland, F.; Downing, J.A. Eutrophication reverses whole-lake carbon budgets. *Inland Waters* **2014**, *4*, 41–48. [CrossRef]
13. Marcon, L.; Schwarz, M.; Backes, L.; Offermann, M.; Schreiber, F.; Hilgert, S.; Sotiri, K.; Jokiel, C.; Lorke, A. Linking Sediment Gas Storage to the Methane Dynamics in a Shallow Freshwater Reservoir. *J. Geophys. Res. Biogeosci.* **2023**, *128*, e2022JG007365. [CrossRef]
14. Gu, B.H.; Schelske, C.L.; Coveney, M.F. Low carbon dioxide partial pressure in a productive subtropical lake. *Aquat. Sci.* **2011**, *73*, 317–330. [CrossRef]
15. Zhou, X.; Jin, F.; Lu, C.; Baoyin, T.; Jia, Z. Shifts in the community composition of methane-cycling microorganisms during lake shrinkage. *Geoderma* **2018**, *311*, 9–14. [CrossRef]
16. Quincey, D.J.; Richardson, S.D.; Luckman, A.; Lucas, R.M.; Reynolds, J.M.; Hambrey, M.J.; Glasser, N.F. Early recognition of glacial lake hazards in the Himalaya using remote sensing datasets. *Glob. Planet. Change* **2007**, *56*, 137–152. [CrossRef]
17. Zhao, R.; Yang, Q.; Wen, Z.; Fang, C.; Li, S.; Shang, Y.; Liu, G.; Tao, H.; Lyu, L.; Song, K. Satellite Estimation of pCO_2 and Quantification of CO_2 Fluxes in China's Chagan Lake in the Context of Climate Change. *Remote Sens.* **2023**, *15*, 5680. [CrossRef]
18. Bastviken, D.; Cole, J.J.; Pace, M.L.; Tranvik, L.J. Methane emissions from lakes: Dependence of lake characteristics, two regional assessments, and a global estimate. *Glob. Biogeochem. Cycles* **2004**, *18*, GB4009. [CrossRef]
19. Bastviken, D.; Cole, J.J.; Pace, M.L.; Van de Bogert, M.C. Fates of methane from different lake habitats: Connecting whole-lake budgets and CH4 emissions. *J. Geophys. Res. Biogeosci.* **2008**, *113*, G02024. [CrossRef]
20. Tranvik, L.J.; Downing, J.A.; Cotner, J.B.; Loiselle, S.A.; Striegl, R.G.; Ballatore, T.J.; Dillon, P.; Finlay, K.; Fortino, K.; Knoll, L.B.; et al. Lakes and reservoirs as regulators of carbon cycling and climate. *Limnol. Oceanogr.* **2009**, *54*, 2298–2314. [CrossRef]
21. Xing, Y.; Xie, P.; Yang, H.; Ni, L.; Wang, Y.; Rong, K. Methane and carbon dioxide fluxes from a shallow hypereutrophic subtropical Lake in China. *Atmos. Environ.* **2005**, *39*, 5532–5540. [CrossRef]
22. Rothfuss, F.; Conrad, R. Effect of gas bubbles on the diffusive flux of methane in anoxic paddy soil. *Limnol. Oceonogr.* **1998**, *43*, 1511–1518. [CrossRef]
23. Martens, C.S.; Klump, J.V. Biogeochemical cycling in an organic-rich coastal marine basin—I. Methane sediment-water exchange processes. *Geochim. Cosmochim. Acta* **1980**, *44*, 471–490. [CrossRef]
24. Yuan, Q.; Valsaraj, K.T.; Reible, D.D.; Willson, C.S. A laboratory study of sediment and contaminant release during gas ebullition. *J. Air Waste Manag. Assoc.* **2007**, *57*, 1103–1111. [CrossRef] [PubMed]
25. Figueiredo-Barros, M.P.-B.; Caliman, A.; Leal, J.J.F.; Bozelli, R.L.; Farjalla, V.F.; Esteves, F.A. Benthic bioturbator enhances CH4 fluxes among aquatic compartments and atmosphere in experimental microcosms. *Can. J. Fish. Aquat. Sci.* **2009**, *66*, 1649–1657. [CrossRef]
26. Brennwald, M.S.; Kipfer, R.; Imboden, D.M. Release of gas bubbles from lake sediment traced by noble gas isotopes in the sediment pore water. Earth Planet. *Sci. Lett.* **2005**, *235*, 31–44. [CrossRef]
27. Klots, C.E. Effect of hydrostatic pressure upon the solubility of gases. *Limnol. Oceanogr.* **1961**, *6*, 365–366. [CrossRef]
28. Jannasch, H.W. Methane oxidation in Lake Kivu (central Africa). *Limnol. Oceanogr.* **1975**, *20*, 860–864. [CrossRef]
29. Strayer, R.F.; Tiedje, J.M. In situ methane production in a small, hypereutrophic, hard-water lake: Loss of methane from sediments by vertical diffusion and ebullition. *Limnol. Oceanogr.* **1978**, *23*, 1201–1206. [CrossRef]
30. Schmiedeskamp, M.; Praetzel, L.S.E.; Bastviken, D.; Knorr, K.H. Whole-lake methane emissions from two temperate shallow lakes with fluctuating water levels: Relevance of spatiotemporal patterns. *Limnol. Oceanogr.* **2021**, *66*, 2455–2469. [CrossRef]
31. Tarasiuk, N.; Koviazina, E.; Kubarevičienė, V.; Shliahtich, E. On the radiocesium carbonate barrier in organics-rich sediments of Lake Juodis, Lithuania. *J. Environ. Radioact.* **2007**, *93*, 100–118. [CrossRef] [PubMed]
32. Meysman, F.J.R.; Malyuga, V.S.; Boudreau, B.P.; Middelburg, J.J. A generalized stochastic approach to particle dispersal in soils and sediments. *Geochim. Cosmochim. Acta* **2008**, *72*, 3460–3478. [CrossRef]
33. Tarasiuk, N.; Špirkauskaitė, N.; Gvozdaitė, R.; Druteikienė, R.; Lukšienė, B. Geophysical problems of radiocesium removal from running shallow lakes. *Environ. Chem. Phys.* **2002**, *24*, 45–60.
34. Koviazina, E.; Tarasiuk, N.; Druteikienė, R.; Gvozdaitė, R. In situ parameterization of self-cleaning from radiocesium in the shallow bottom terrace of Lake Juodis. *Environ. Chem. Phys.* **2003**, *25*, 123–128.

35. Tarasiuk, N.; Moisejenkova, A.; Koviazina, E. On the mechanism of the enrichment in radiocesium of near-bottom water in Lake Juodis, Lithuania. *J. Environ. Radioact.* **2010**, *101*, 883–894. [CrossRef] [PubMed]
36. Tarasiuk, N.; Koviazina, E.; Schliahtič, E. On the optimization of empirical data concerning radionuclides in water of Lake Juodis. *Environ. Chem. Phys.* **2004**, *24*, 118–128.
37. Bazhin, N.M. Theoretical consideration of methane emission from sediments. *Chemosphere* **2003**, *50*, 191–200. [CrossRef]
38. Chanton, J.P.; Martens, C.S.; Kelley, C.A. Gas transport from methane-saturated, tidal freshwater and wetland sediments. *Limnol. Oceanogr.* **1989**, *34*, 807–819. [CrossRef]
39. Casper, P.; Maberly, S.C.; Hall, G.H.; Finlay, B.J. Fluxes of methane and carbon dioxide from a small productive lake to the atmosphere. *Biogeochemistry* **2000**, *49*, 1–19. [CrossRef]
40. Natchimuthu, S.; Sundgren, I.; Gålfalk, M.; Klemedtsson, L.; Crill, P.; Danielsson, Å.; Bastviken, D. Spatio-temporal variability of lake CH4 fluxes and its influence on annual whole lake emission estimates. *Limnol. Oceanogr.* **2016**, *61*, S13–S26. [CrossRef]